Application of the dynamic condensation approach to the hybrid FE-SEA model of mid-frequency vibration in complex built-up systems

Ruxin Gao[a], Yahui Zhang[a*], David Kennedy[b]

[a] *State Key Laboratory of Structural Analysis for Industrial Equipment, Department of Engineering Mechanics, International Center for Computational Mechanics, Dalian University of Technology, Dalian 116023, PR China;*

[b] *School of Engineering, Cardiff University, Cardiff CF24 3AA, Wales, UK*

Corresponding author:

Dr. Y. H. Zhang

State Key Laboratory of Structural Analysis for Industrial Equipment, Department of Engineering Mechanics, Dalian University of Technology, Dalian 116023, PR China

Email: zhangyh@dlut.edu.cn

Tel: +86 411 84706337

Fax: +86 411 84708393

Abstract

The hybrid Finite Element (FE) - Statistical Energy Analysis (SEA) method developed for mid-frequency vibration of complex built-up systems needs to compute the total dynamic flexibility matrix at every frequency, which is very time consuming. This paper presents an improved hybrid FE-SEA method to overcome this problem. In the present method, first, dynamic condensation is introduced to reduce the order of the deterministic FE component, which results in significant reduction of the total dynamic stiffness matrix. Then, noting that the dynamic stiffness matrix of the deterministic component is established by using the FE method, a fast inverse algorithm is employed to calculate the dynamic flexibility matrix of the slave degrees of freedom of the deterministic component generated in the condensation process. These two steps avoid the direct inverse computation of a large matrix at each frequency point of interest, resulting in significant time saving. A numerical example illustrates the efficiency and convergence of the proposed method.

Keywords: Mid-frequency; Complex built-up systems; Hybrid FE-SEA method; Dynamic condensation approach; Dynamic flexibility

1 Introduction

In general, dynamic analysis methods for mechanical systems may be divided into two types: deterministic analysis methods for low-frequency vibration and statistical methods for high-frequency vibration. The first type, such as the Finite Element (FE) method [1] and Boundary Element (BE) method [2], is suitable for the so-called deterministic system whose nominal geometric and material parameters are clearly known and which has only a few low-order modes (of long wavelength deformation) in the frequency range of interest. The second type, such as Statistical Energy Analysis (SEA) [3], is suitable for the so-called statistical system whose nominal geometric and material parameters may not be clearly known and which has many high-order modes (of short wavelength deformation) in the frequency range of interest.

A complex built-up system, however, may be composed of many components which have significantly different dynamic behaviors at high frequencies due to the different properties of geometries and materials. Some components may be subjected to long wavelength deformation and have lower modal density, while other components may be subjected to short wavelength deformation and have higher modal density. Such mixed dynamic behavior is the so-called mid-frequency vibration of complex built-up systems [4, 5]. In this case, a deterministic method, such as the FE method, requires many degrees of freedom to model the system and the response may be very sensitive to small imperfections in the system [4, 5]. A statistical method such as SEA, which is

developed based on the assumption of high modal density, may generate an unacceptable error due to the high modal densities of some components [4, 5]. Hence, the complex built-up system may not be well modelled using a single deterministic or statistical method. To solve the above problems, many improved methods have been developed with the aim of extending the effective frequency range of deterministic methods [6-13] and addressing the applicability of the assumptions of statistical methods [14-20]. In addition, a widely studied hybrid approach [21-27] combines the deterministic and statistical methods to establish a hybrid model which can describe the response of the complex built-up system more efficiently.

Considering the different vibration behaviors of the components of the complex built-up system, the hybrid approach employs a deterministic method to model the components which are subjected to long wavelength deformation (that is, the so-called deterministic subsystem) and a statistical method to model the components which are subjected to short wavelength deformation (that is, the so-called statistical subsystem). It establishes a non-iterative relationship between the deterministic and statistical subsystems by using the diffuse-field reciprocity [28]. Among all the hybrid approaches, one of the most representative is the hybrid FE-SEA method [22-23,29]. Based on the framework of the hybrid FE-SEA method, many other hybrid formats [24-27] for specific problems were developed to improve computational efficiency through modelling the deterministic subsystem using other deterministic methods instead of FE.

It is important to point out, however, that thanks to the strong applicability of FE, in the hybrid FE-SEA method the structural matrices of the deterministic subsystem (i.e. the mass, stiffness and damping matrices) are frequency-independent, and the total dynamic stiffness matrix is sparse and symmetric and can be solved easily. Furthermore, for deterministic subsystems with complex shapes or boundaries, the hybrid FE-SEA method is almost irreplaceable.

It should be noted that the hybrid FE-SEA method needs to compute the inverse of the total dynamic stiffness matrix at every frequency, which is very time consuming. Although the inverse matrix may be obtained analytically, solving large linear systems with multiple right-hand sides is very difficult and time expensive. In addition, the governing equation employed in the hybrid FE-SEA method is established based on the hybrid model, not a pure FE model, so the condensation approach and fast inverse algorithms developed based on the pure FE model cannot be used directly in the hybrid FE-SEA method.

In this paper, the order of the deterministic subsystem is first reduced by using traditional condensation, and so the size of the total dynamic stiffness matrix is indirectly reduced. Then, although another inverse matrix (the dynamic flexibility matrix of the slave degrees of freedom of the deterministic subsystem) needs to be calculated in the dynamic condensation process, because the deterministic subsystem is modelled using a pure FE model, not a hybrid model, a fast algorithm proposed by

Leung [30] can be introduced here to obtain this inverse matrix. Avoiding the direct inversion of a large matrix at each frequency, the present method, of course, greatly improves the calculation efficiency and reduces the computation time. Section 2 outlines the basic principles of the hybrid FE-SEA method and gives some discussion about its efficiency. Section 3 shows the application of the dynamic condensation approach to the hybrid FE-SEA method, followed by formulations of the fast inverse algorithm for the dynamic flexibility matrix of the slave degrees of freedom of the deterministic subsystem. In section 4, a numerical example illustrates the efficiency and the convergence of the present method. Conclusions are given in section 5.

2 Basic principles of the hybrid method

According to the hybrid FE-SEA method [22], a complex built-up system can be divided into two parts: the deterministic and statistical subsystems. The response of the statistical subsystem is viewed as the superposition of the direct and reverberant fields, which respectively generate the direct field dynamic stiffness matrix and the blocked reverberant force [22, 28]. In the hybrid FE-SEA method, considering the effect of the direct stiffness matrix and the blocked reverberant force, the governing equation of the deterministic subsystem can firstly be established. Then the power balance equation for the statistical subsystem can be found by considering the conservation of energy. Finally, the governing and power balance equations are connected by the diffuse-field

reciprocity relationship [28]. The above three steps establish a non-iterative hybrid method for the mid-frequency vibration of complex built-up systems.

2.1 Governing equation of the deterministic subsystem

The deterministic component is subjected to the forces $\mathbf{f}_{\mathrm{dir}}^{(j)}$ and $\mathbf{f}_{\mathrm{rev}}^{(j)}$, respectively generated from the direct and reverberant fields of the jth statistical component. The governing equation for the deterministic component can be written as [22]

$$\mathbf{D}_{\mathrm{d}}\mathbf{q} = \mathbf{f}_{\mathrm{ext}} + \sum_{j}\mathbf{f}_{\mathrm{rev}}^{(j)} - \sum_{j}\mathbf{f}_{\mathrm{dir}}^{(j)} \tag{1}$$

where $\mathbf{q}$ represents the degrees of freedom of the deterministic component, $\mathbf{f}_{\mathrm{ext}}$ is the vector of generalized forces acting on the deterministic component. $\mathbf{D}_{\mathrm{d}}$ represents the dynamic stiffness matrix of the deterministic component and can be expressed as

$$\mathbf{D}_{\mathrm{d}} = -\omega^2\mathbf{M}_{\mathrm{d}} + \mathrm{i}\omega\mathbf{C}_{\mathrm{d}} + \mathbf{K}_{\mathrm{d}} \tag{2}$$

where $\mathbf{K}_{\mathrm{d}}$, $\mathbf{M}_{\mathrm{d}}$ and $\mathbf{C}_{\mathrm{d}}$ respectively represent the stiffness, mass and damping matrices of the deterministic component. ω and i are the angular frequency and imaginary unit, respectively.

Considering the equilibrium of the direct field forces of the jth statistical component, $\mathbf{f}_{\mathrm{dir}}^{(j)}$ can be expressed in terms of the direct field dynamic stiffness matrix $\mathbf{D}_{\mathrm{dir}}^{(j)}$ and the vector of degrees of freedom $\mathbf{q}$ as [22]

$$\mathbf{f}_{\mathrm{dir}}^{(j)} = \mathbf{D}_{\mathrm{dir}}^{(j)}\mathbf{q} \tag{3}$$

Inserting Eq. (3) into Eq. (1), the governing equation of the deterministic subsystem can be written as [22]

$$\mathbf{D}_{\mathrm{tot}}\mathbf{q} = \mathbf{f}_{\mathrm{ext}} + \sum_j \mathbf{f}_{\mathrm{rev}}^{(j)} \tag{4}$$

where

$$\mathbf{D}_{\mathrm{tot}} = \mathbf{D}_{\mathrm{d}} + \sum_j \mathbf{D}_{\mathrm{dir}}^{(j)} \tag{5}$$

represents the total dynamic stiffness matrix.

2.2 Power balance equation of the statistical subsystems

Assuming that the statistical subsystem has sufficient uncertainty, the blocked reverberant force equals zero [22]. Rewriting Eq. (4) in cross-spectral form and averaging over a random ensemble of statistical subsystems gives

$$\mathbf{S}_{qq} = \mathbf{S}_{qq}^{\mathrm{ext}} + \mathbf{S}_{qq}^{\mathrm{rev}} \tag{6}$$

where $\mathbf{S}_{qq}$ is the cross-spectral matrix of the displacement vector $\mathbf{q}$, and

$$\mathbf{S}_{qq}^{\mathrm{ext}} = \mathbf{D}_{\mathrm{tot}}^{-1}\mathbf{S}_{ff}^{\mathrm{ext}}\mathbf{D}_{\mathrm{tot}}^{-\mathrm{H}} \tag{7}$$

$$\mathbf{S}_{qq}^{\mathrm{rev}} = \mathbf{D}_{\mathrm{tot}}^{-1}\mathbf{S}_{ff}^{\mathrm{rev}}\mathbf{D}_{\mathrm{tot}}^{-\mathrm{H}} \tag{8}$$

where $\mathbf{S}_{ff}^{ext} = \langle \mathbf{f}_{ext} \mathbf{f}_{ext}^{H} \rangle$ and $\mathbf{S}_{ff}^{rev} = \sum_j \langle \mathbf{f}_{rev}^{(j)} \mathbf{f}_{rev}^{(j),H} \rangle$ are the cross-spectral matrices of the external and blocked reverberant forces, respectively. $\#^{H}$ is the complex Hermitian transpose of $\#$, $\#^{-H}$ is the complex Hermitian transpose of the inverse of $\#$ and $\langle \# \rangle$ represents the ensemble average. According to the diffuse-field reciprocity [28], $\mathbf{S}_{ff}^{rev}$ can be expressed in terms of the energy of the statistical subsystem

$$\mathbf{S}_{ff}^{rev} = \sum_j \alpha_j \mathrm{Im}\{\mathbf{D}_{dir}^{(j)}\} \tag{9}$$

where

$$\alpha_j = \frac{4E_j}{\pi \omega n_j} \tag{10}$$

and n_j and E_j are the modal density and ensemble average energy of the jth statistical subsystem. For the sake of simplicity, Eq. (8) can be rewritten as

$$\mathbf{S}_{qq}^{rev} = \sum_j \alpha_j \mathbf{Y}_{dir}^{(j)} \tag{11}$$

where

$$\mathbf{Y}_{dir}^{(j)} = \mathbf{D}_{tot}^{-1} \mathrm{Im}\{\mathbf{D}_{dir}^{(j)}\} \mathbf{D}_{tot}^{-H} \tag{12}$$

The statistical subsystems are modelled using SEA. Considering the energy conservation of the statistical subsystems, the power balance equations of all statistical

subsystems can be written as [3]

$$\mathbf{L}\mathbf{N}^{-1}\mathbf{E} = \mathbf{P}_{\text{in}}^{\text{ext}} + \mathbf{P}_{\text{in}}^{\text{dir}} \tag{13}$$

where $\mathbf{L}$ is the influence matrix of the modal energy, $\mathbf{N}$ is a diagonal matrix with the modal densities on main diagonal and $\mathbf{E}$ represents the time and ensemble average energy of the statistical subsystems. $\mathbf{P}_{\text{in}}^{\text{ext}}$ and $\mathbf{P}_{\text{in}}^{\text{dir}}$ are the time and ensemble average input power to the statistical subsystems due to the presence of the external force and deterministic subsystem. Ref. [22] gives a detailed derivation of Eq. (13).

The energy of each statistical subsystem can be obtained by solving the power balance equation (13). Then, the cross-spectral response of the deterministic subsystem can be obtained by inserting the energy into Eqs. (6)-(8).

2.3 Discussion of computational efficiency

As can be seen from Eqs. (7) and (12), the hybrid FE-SEA method requires computation of the inverse of the total dynamic stiffness matrix at every frequency. Although such a matrix can be obtained analytically, it is very difficult and time consuming to solve large linear systems with multiple right-hand sides, and it gets worse as the number of the degrees of freedom increases. In addition, since the direct field dynamic stiffness matrix is generally calculated using the BE method [28], the matrix coefficients in BE method are frequency dependent. As a result, the extraction of the natural frequencies of the direct field cannot be realized by an algebraic eigenvalue

problem. Since the total dynamic stiffness matrix is the sum of the dynamic stiffness matrices of the deterministic component and the direct field, the extraction of the natural frequencies of the deterministic subsystem also cannot be realized by an algebraic eigenvalues problem. Hence, fast inverse algorithms [30] developed based on the pure FE method cannot be used directly to calculate the inverse of the total dynamic stiffness matrix.

In order to solve the above problem and improve the computational efficiency of the hybrid FE-SEA method, this paper presents an improved solution strategy. The proposed method employs the dynamic condensation approach to reduce the degrees of freedom of the deterministic component. As a result, the order of the total dynamic stiffness matrix can be indirectly, but significantly, reduced without loss of accuracy. It should be noted that another inverse matrix, i.e. the inverse matrix of the dynamic stiffness matrix of the slave degrees of freedom of the deterministic component, needs to be calculated in the condensation process. Since the deterministic component is modelled using the FE method, this matrix can be obtained by using a fast inverse algorithm [30], by which the inverse of the dynamic stiffness matrix of a pure FE model can be calculated, using only matrix multiplication or addition between the frequency-independent structural matrices (the stiffness, mass and damping matrices), without any matrix inversion operations. Although the fast inverse algorithm will introduce some small errors, the computational efficiency can be improved significantly with an

acceptable accuracy.

3 Application of the dynamic condensation approach to the hybrid FE-SEA model

3.1 Dynamic condensation of the statistical component

According to the basic principle of the dynamic condensation approach [30], all the degrees of freedom of the deterministic component can be divided into two types, i.e. master and slave degrees of freedom. The degrees of freedom located at the junction and the area of the external excitation are defined as the master degrees of freedom, while the degrees of freedom located elsewhere are defined as slave degrees of freedom. Ordering the displacement vector according to the master and slave degrees of freedom gives $\tilde{\mathbf{q}} = \bar{\mathbf{T}}^{\mathrm{T}}\mathbf{q}$, where $\bar{\mathbf{T}}$ represents a permutation matrix with $\bar{\mathbf{T}}\bar{\mathbf{T}}^{\mathrm{T}} = \mathbf{I}$ and $\#^{\mathrm{T}}$ is the transpose of #. Then the displacement vector $\mathbf{q}$ can be written as

$$\mathbf{q} = \bar{\mathbf{T}}\tilde{\mathbf{q}} = \bar{\mathbf{T}}\begin{Bmatrix}\mathbf{q}^{\mathrm{m}}\\ \mathbf{q}^{\mathrm{s}}\end{Bmatrix} \tag{14}$$

where superscripts m and s respectively represent the master and slave degrees of freedom. Inserting Eq. (14) into Eq. (4) and pre-multiplying by $\bar{\mathbf{T}}^{\mathrm{T}}$ gives

$$\tilde{\mathbf{D}}_{\mathrm{tot}}\tilde{\mathbf{q}} = \tilde{\mathbf{f}}_{\mathrm{ext}} + \sum_{j}\tilde{\mathbf{f}}_{\mathrm{rev}}^{(j)} \tag{15}$$

where

$$\tilde{\mathbf{D}}_{\text{tot}} = \tilde{\mathbf{T}}^{\text{T}} \mathbf{D}_{\text{tot}} \tilde{\mathbf{T}} = \begin{bmatrix} \mathbf{D}_{\text{tot}}^{\text{mm}} & \mathbf{D}_{\text{tot}}^{\text{ms}} \\ \mathbf{D}_{\text{tot}}^{\text{sm}} & \mathbf{D}_{\text{tot}}^{\text{ss}} \end{bmatrix} \tag{16}$$

$$\tilde{\mathbf{f}}_{\text{ext}} = \tilde{\mathbf{T}}^{\text{T}} \mathbf{f}_{\text{ext}} = \begin{Bmatrix} \mathbf{f}_{\text{ext}}^{\text{m}} \\ \mathbf{f}_{\text{ext}}^{\text{s}} \end{Bmatrix} \tag{17}$$

$$\tilde{\mathbf{f}}_{\text{rev}}^{(j)} = \tilde{\mathbf{T}}^{\text{T}} \mathbf{f}_{\text{rev}}^{(j)} = \begin{Bmatrix} \mathbf{f}_{\text{rev}}^{(j),\text{m}} \\ \mathbf{f}_{\text{rev}}^{(j),\text{s}} \end{Bmatrix} \tag{18}$$

Since the master degrees of freedom lie on the junction and the area of the external excitation, it is clear that $\mathbf{f}_{\text{ext}}^{\text{s}} = \mathbf{0}$, $\mathbf{f}_{\text{rev}}^{(j),\text{s}} = \mathbf{0}$, $\mathbf{D}_{\text{dir}}^{(j),\text{ss}} = \mathbf{0}$, $\mathbf{D}_{\text{dir}}^{(j),\text{ms}} = \mathbf{0}$, $\mathbf{D}_{\text{dir}}^{(j),\text{sm}} = \mathbf{0}$. As a result, using Eqs. (15)-(18), a relationship between the master and slave degrees of freedom can be written as

$$\mathbf{q}^{\text{s}} = \mathbf{T}\mathbf{q}^{\text{m}} \tag{19}$$

where

$$\mathbf{T} = -\mathbf{D}_{\text{d}}^{\text{ss}\,-1} \mathbf{D}_{\text{d}}^{\text{sm}} \tag{20}$$

Hence, Eq. (15) can be reduced to

$$\mathbf{D}_{\text{m}} \mathbf{q}^{\text{m}} = \mathbf{f}_{\text{ext}}^{\text{m}} + \sum_{j} \mathbf{f}_{\text{rev}}^{(j),\text{m}} \tag{21}$$

where

$$\mathbf{D}_{\mathrm{m}} = \mathbf{D}_{\mathrm{d}}^{\mathrm{mm}} + \sum_{j} \mathbf{D}^{(j)}{}_{\mathrm{dir}}^{\mathrm{mm}} + \mathbf{D}_{\mathrm{d}}^{\mathrm{ms}}\mathbf{T} \tag{22}$$

Comparing with the original governing Eq. (4), the reduced governing Eq. (21) has a similar form, but fewer degrees of freedom and higher efficiency. As mentioned in section 2.3, theoretically there is no loss of accuracy from Eq. (4) to Eq. (21).

The displacement cross-spectrum of the master degrees of freedom, $\boldsymbol{S}_{qq}^{\mathrm{mm}}$, can be obtained by using an analogous analysis to that in Eqs. (6)-(13). Furthermore, by using Eqs. (14) and (19), the cross-spectrum matrix of the original displacement, $\boldsymbol{S}_{qq}$, can be written as

$$\boldsymbol{S}_{qq} = \tilde{\mathbf{T}}\boldsymbol{S}_{\tilde{q}\tilde{q}}\tilde{\mathbf{T}}^{\mathrm{T}} = \tilde{\mathbf{T}}\begin{bmatrix} \boldsymbol{S}_{qq}^{\mathrm{mm}} & \boldsymbol{S}_{qq}^{\mathrm{ms}} \\ \boldsymbol{S}_{qq}^{\mathrm{sm}} & \boldsymbol{S}_{qq}^{\mathrm{ss}} \end{bmatrix}\tilde{\mathbf{T}}^{\mathrm{T}} \tag{23}$$

where

$$\boldsymbol{S}_{qq}^{\mathrm{ss}} = \mathbf{T}\boldsymbol{S}_{qq}^{\mathrm{mm}}\mathbf{T}^{\mathrm{T}},\ \boldsymbol{S}_{qq}^{\mathrm{ms}} = \boldsymbol{S}_{qq}^{\mathrm{mm}}\mathbf{T}^{\mathrm{T}},\ \boldsymbol{S}_{qq}^{\mathrm{sm}} = \mathbf{T}\boldsymbol{S}_{qq}^{\mathrm{mm}} \tag{24}$$

3.2 Fast inverse algorithm for dynamic stiffness calculation

It can be seen from Eq. (20) that another inverse matrix needs to be calculated in the condensation process. The fewer master degrees of freedom are selected, the larger the order of the matrix $\mathbf{D}_{\mathrm{d}}^{\mathrm{ss}}$. In fact, the dynamic condensation approach transfers the expensive computation from one inversion operation to another. The latter, however, can be realized by using the fast inverse algorithm.

As in Eq. (2), $\mathbf{D}_{\mathrm{d}}^{ss}$ can be written as

$$\mathbf{D}_{\mathrm{d}}^{ss} = -\omega^2\mathbf{M}_{\mathrm{d}}^{ss} + \mathrm{i}\omega\mathbf{C}_{\mathrm{d}}^{ss} + \mathbf{K}_{\mathrm{d}}^{ss} \tag{25}$$

where $\mathbf{K}_{\mathrm{d}}^{ss}$, $\mathbf{M}_{\mathrm{d}}^{ss}$ and $\mathbf{C}_{\mathrm{d}}^{ss}$ respectively represent the ordered stiffness, mass and damping matrices of the slave degrees of freedom of the deterministic component. Depending on the existence of the damping matrix, the fast inverse algorithm [30] for the dynamic flexibility matrix $\mathbf{Z}_{\mathrm{d}}^{ss} = \mathbf{D}_{\mathrm{d}}^{ss\,-1}$ may be introduced for two cases, as follows.

Firstly, for the case of $\mathbf{C}_{\mathrm{d}}^{ss} = \mathbf{0}$, Eq. (25) can be rewritten as $\mathbf{D}_{\mathrm{d}}^{ss} = -\omega^2\mathbf{M}_{\mathrm{d}}^{ss} + \mathbf{K}_{\mathrm{d}}^{ss}$. Performing generalized eigenvalue decomposition for $\mathbf{K}_{\mathrm{d}}^{ss}$ and $\mathbf{M}_{\mathrm{d}}^{ss}$, one can obtain the fixed interface modal matrix $\boldsymbol{\Phi}$ and a diagonal matrix $\boldsymbol{\Omega}^2$, with

$$\boldsymbol{\Phi}^{\mathrm{T}}\mathbf{M}_{\mathrm{d}}^{ss}\boldsymbol{\Phi} = \mathbf{I} \tag{26}$$

$$\boldsymbol{\Phi}^{\mathrm{T}}\mathbf{K}_{\mathrm{d}}^{ss}\boldsymbol{\Phi} = \boldsymbol{\Omega}^2 \tag{27}$$

Pre- and post-multiplying Eq. (25) by $\boldsymbol{\Phi}^{\mathrm{T}}$ and $\boldsymbol{\Phi}$, respectively, and noting that $\mathbf{C}_{\mathrm{d}}^{ss} = \mathbf{0}$, gives

$$\boldsymbol{\Phi}^{\mathrm{T}}\mathbf{D}_{\mathrm{d}}^{ss}\boldsymbol{\Phi} = \left(\boldsymbol{\Omega}^2 - \omega^2\mathbf{I}\right) \tag{28}$$

Performing the inversion operation on Eq. (28) gives

$$\boldsymbol{\Phi}^{-1}\mathbf{D}_{\mathrm{d}}^{ss\,-1}\boldsymbol{\Phi}^{-\mathrm{T}} = (\boldsymbol{\Omega}^2 - \omega^2\mathbf{I})^{-1} \tag{29}$$

where $\#^{-\mathrm{T}}$ represents the transpose of the inverse of #. Using Eq. (29), $\mathbf{Z}_{\mathrm{d}}^{ss}$ can be easily obtained and written as

$$\mathbf{Z}_{\mathrm{d}}^{ss} = \mathbf{D}_{\mathrm{d}}^{ss\,-1} = \boldsymbol{\Phi}(\boldsymbol{\Omega}^2 - \omega^2\mathbf{I})^{-1}\boldsymbol{\Phi}^{\mathrm{T}} \tag{30}$$

Because $(\boldsymbol{\Omega}^2 - \omega^2\mathbf{I})$ is a diagonal matrix, its inverse can be easily calculated. It should be noted that there is a loss of accuracy in Eq. (30) resulting from mode truncation, and as Ref. [30] pointed out, Eq. (30) has a very slow convergence rate. However, accelerated convergence can be achieved using the following formula.

$$(\boldsymbol{\Omega}^2 - \omega^2\mathbf{I})^{-1} = \boldsymbol{\Omega}^{-2} + \omega^2\boldsymbol{\Omega}^{-4} + \cdots + \omega^{2j-2}\boldsymbol{\Omega}^{-2j} + \omega^{2j}\boldsymbol{\Omega}^{-2j}(\boldsymbol{\Omega}^2 - \omega^2\mathbf{I})^{-1} \quad (31)$$
$$= 1,2,\cdots$$

The above formula is exact for any positive integer j. Generally, taking $j = 2$ can obtain a good convergence rate. Inserting Eq. (31) into Eq. (30) gives (for $j = 2$)

$$\mathbf{Z}_{\mathrm{d}}^{ss} = \mathbf{K}_{\mathrm{d}}^{ss\,-1} + \omega^2\mathbf{K}_{\mathrm{d}}^{ss\,-1}\mathbf{M}_{\mathrm{d}}^{ss}\mathbf{K}_{\mathrm{d}}^{ss\,-1} + \omega^4\boldsymbol{\Phi}\boldsymbol{\Omega}^{-4}(\boldsymbol{\Omega}^2 - \omega^2\mathbf{I})^{-1}\boldsymbol{\Phi}^{\mathrm{T}} \tag{32}$$

The loss of accuracy in Eq. (32) also comes from mode truncation. Comparing to Eq. (30), however, Eq. (32) has a faster convergence rate.

Secondly, for the case of $\mathbf{C}_{\mathrm{d}}^{ss} \neq \mathbf{0}$, Eq. (25) can be rewritten as $\mathbf{D}_{\mathrm{d}}^{ss}(\lambda) = \lambda^2\mathbf{M}_{\mathrm{d}}^{ss} + \lambda\mathbf{C}_{\mathrm{d}}^{ss} + \mathbf{K}_{\mathrm{d}}^{ss}$, by setting $\lambda = \mathrm{i}\omega$. Performing complex generalized eigenvalue decomposition, one can obtain the fixed interface complex modal matrix $\boldsymbol{\Psi}$ and a

diagonal matrix $\mathbf{\Lambda}$. Employing the Taylor series expansion of $\mathbf{Z}_{\mathrm{d}}^{ss}(\lambda)$ about $\lambda = 0$, $\mathbf{Z}_{\mathrm{d}}^{ss}(\lambda)$ can be expressed as [30]

$$\mathbf{Z}_{\mathrm{d}}^{ss}(\lambda) = \mathbf{Z}_{\mathrm{d}}^{ss}(0) + \lambda \mathbf{Z}_{\mathrm{d}}^{ss\,'}(0) + \frac{1}{2}\lambda^2 \mathbf{Z}_{\mathrm{d}}^{ss\,''}(0) + \frac{1}{6}\lambda^3 \mathbf{Z}_{\mathrm{d}}^{ss\,'''}(0) + \lambda^4 \mathbf{\Psi}\mathbf{\Lambda}^{-4}(\lambda \mathbf{I} \qquad (33)$$

where superscript primes stand for derivatives with respect to λ. Similar to Eq. (32), the loss of accuracy in Eq. (33) comes from complex mode truncation. Performing successive differentiation to $\mathbf{D}_{\mathrm{d}}^{ss}\mathbf{Z}_{\mathrm{d}}^{ss} = \mathbf{I}$ yields

$$\mathbf{Z}_{\mathrm{d}}^{ss\,'}\mathbf{D}_{\mathrm{d}}^{ss} + \mathbf{Z}_{\mathrm{d}}^{ss}\mathbf{D}_{\mathrm{d}}^{ss\,'} = \mathbf{0} \qquad (34)$$

$$\mathbf{Z}_{\mathrm{d}}^{ss\,''}\mathbf{D}_{\mathrm{d}}^{ss} + 2\mathbf{Z}_{\mathrm{d}}^{ss\,'}\mathbf{D}_{\mathrm{d}}^{ss\,'} + \mathbf{Z}_{\mathrm{d}}^{ss}\mathbf{D}_{\mathrm{d}}^{ss\,''} = \mathbf{0} \qquad (35)$$

$$\mathbf{Z}_{\mathrm{d}}^{ss\,'''}\mathbf{D}_{\mathrm{d}}^{ss} + 3\mathbf{Z}_{\mathrm{d}}^{ss\,''}\mathbf{D}_{\mathrm{d}}^{ss\,'} + 3\mathbf{Z}_{\mathrm{d}}^{ss\,'}\mathbf{D}_{\mathrm{tot}}^{ss\,''} + \mathbf{Z}_{\mathrm{d}}^{ss}\mathbf{D}_{\mathrm{d}}^{ss\,'''} = \mathbf{0} \qquad (36)$$

The derivatives of $\mathbf{Z}_{\mathrm{d}}^{ss}$ with respect to λ can thus be calculated from Eqs. (34)-(36). Inserting $\lambda = 0$ into those derivatives yields

$$\mathbf{Z}_{\mathrm{d}}^{ss}(0) = \mathbf{K}_{\mathrm{d}}^{ss\,-1} \qquad (37)$$

$$\mathbf{Z}_{\mathrm{d}}^{ss\,'}(0) = -\mathbf{K}_{\mathrm{d}}^{ss\,-1}\mathbf{C}_{\mathrm{d}}^{ss}\mathbf{K}_{\mathrm{d}}^{ss\,-1} \qquad (38)$$

$$\mathbf{Z}_{\mathrm{d}}^{ss\,''}(0) = 2\left(\mathbf{K}_{\mathrm{d}}^{ss\,-1}\left(\mathbf{C}_{\mathrm{d}}^{ss}\mathbf{K}_{\mathrm{d}}^{ss\,-1}\right)^2 - \mathbf{K}_{\mathrm{d}}^{ss\,-1}\mathbf{M}_{\mathrm{d}}^{ss}\mathbf{K}_{\mathrm{d}}^{ss\,-1}\right) \qquad (39)$$

$$\mathbf{Z}_{\mathrm{d}}^{ss'''}(0) = -6\left(\mathbf{K}_{\mathrm{d}}^{ss-1}\left(\mathbf{C}_{\mathrm{d}}^{ss}\mathbf{K}_{\mathrm{d}}^{ss-1}\right)^{3} - \mathbf{K}_{\mathrm{d}}^{ss-1}\mathbf{C}_{\mathrm{d}}^{ss}\mathbf{K}_{\mathrm{d}}^{ss-1}\mathbf{M}_{\mathrm{d}}^{ss}\mathbf{K}_{\mathrm{d}}^{ss-1} - \mathbf{K}_{\mathrm{d}}^{ss-1}\mathbf{M}_{\mathrm{d}}^{ss}\mathbf{K}_{\mathrm{d}}^{ss-1}\mathbf{C}_{\mathrm{d}}^{ss}\mathbf{K}\right. \tag{40}$$

Inserting Eqs. (37)-(40) into Eq. (33), $\mathbf{Z}_{\mathrm{d}}^{ss}$ can be obtained without direct inversion operations. Moreover, it can be seen from Eqs. (37)-(40) that Eq. (33) reduces to Eq. (32) if $\mathbf{C}_{\mathrm{d}}^{ss} = \mathbf{0}$.

4 Numerical example

A validation example from Ref. [29], as shown in Fig. 1, is included here to illustrate the efficiency and convergence of the proposed method. This complex built-up system consists of four thin panels and a beam framework. Each panel is bolted to the beam framework at four points with an offset of 17mm to the neutral axis of the beams. All panels are made of aluminium (density $\rho_s = 2700$ kg/m^3, Young's modulus $E = 71$ GPa, Poisson's ratio $\nu = 0.33$, loss factor $\eta = 0.01$) and they each have dimensions 0.6m×1.1m×1mm. The beams that make up the framework are also made of aluminium and they form the edges of a cube. Each beam is 0.7m long, with a square hollow section whose external side width and wall thickness are 25.4mm and 3.2mm, respectively. All plain cylindrical bolts used to connect the panels and framework have a radius of 5mm, and the distance between two successive bolts on a same beam is 0.2m. A unit point force is applied in the vertical direction on one of the bottom beams at 0.25m from the corner, as shown in Fig. 1 (#1). The frequency range considered here

is from 50Hz to 300Hz with a frequency step of 1Hz. The excitation point, #1, is selected as the first observation point. The second observation point, #2, is on one of the top beams at 0.25m from the corner, and the horizontal direction is selected as shown in Fig. 1.

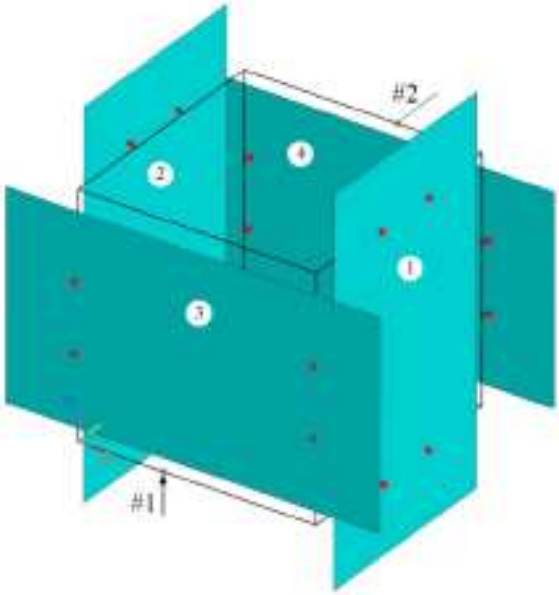

Fig. 1 A framework-panel system.

The reference results are obtained using the previous hybrid FE-SEA method, which employs the same hybrid FE-SEA model as the proposed method. The partition of the system can be obtained based on the free propagating wavelengths across the given frequency band. In the panels, the shear and extensional wavelengths are both greater than 15m at 300Hz, indicating that the in-plane motion should be modelled using FE, while the bending wavelength is 0.31m and 0.18m at 100Hz and 300Hz,

respectively, suggesting that the out-plane motion should be modelled using SEA. Performing similar analysis to the beams that make up the framework, it is inferred that the framework should be modelled using FE [29].

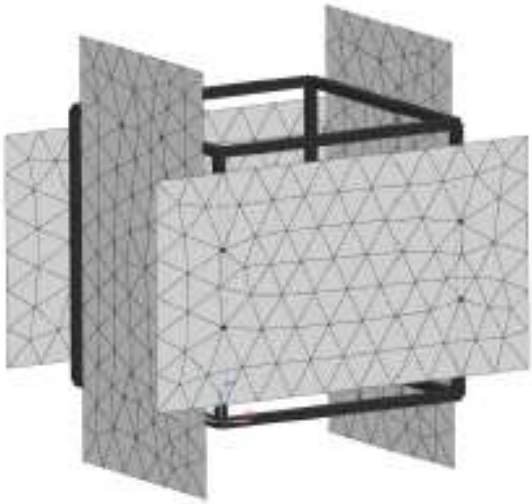

Fig. 2 Finite element mesh of the deterministic subsystem of a framework-panel system.

The FE model used in the two methods is shown in Fig. 2. It consists of 352 CBEAM [31] elements and 652 CTRIA3 [31] elements, with a total of 2852 degrees of freedom. The degrees of freedom corresponding to the deterministic component, excitation and observation points are selected to be the master degrees of freedom, illustrating that the reduced model employed in the proposed method has only 18 master degrees of freedom.

In order to verify the validity and efficiency of the proposed method, the responses of the system were calculated by employing the previous hybrid FE-SEA method and

the proposed method under 150 included modes. Figs. 3-6 show the energies of the four panels obtained by the two methods, while Figs. 7-8 show the velocity squared frequency response at observation points #1 and #2. A good agreement between the two methods can be seen from Figs. 3-8. It should be pointed out that the results obtained using the proposed method with only the dynamic condensation approach, but without the fast inverse algorithm, are in theory exactly the same as those obtained using the previous hybrid FE-SEA method.

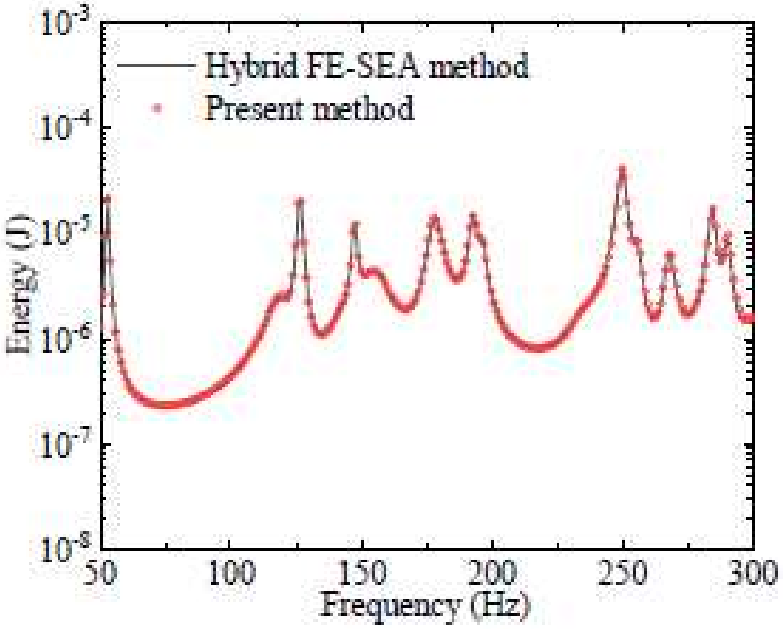

Fig. 3 Energy in panel 1.

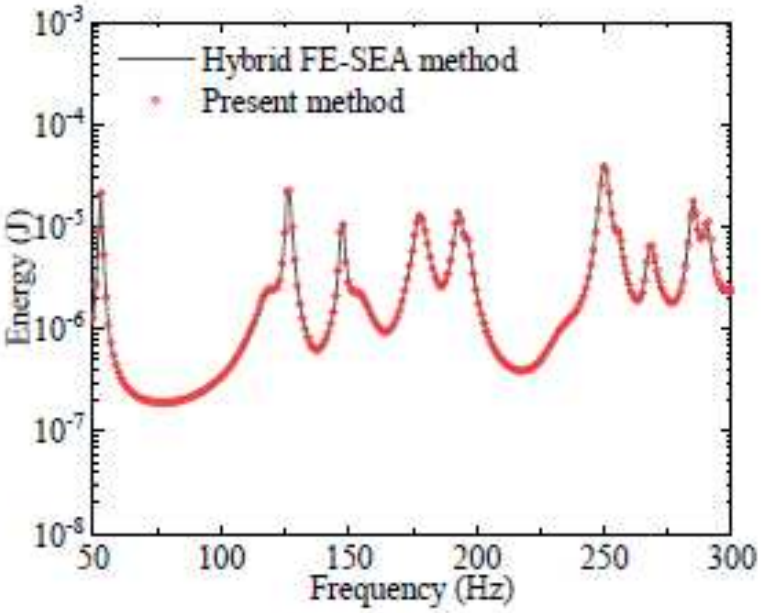

Fig. 4 Energy in panel 2.

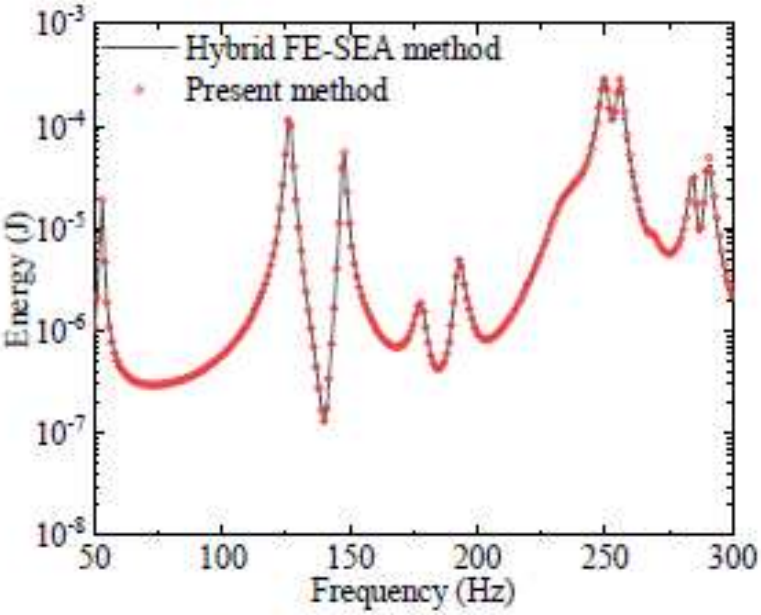

Fig. 5 Energy in panel 3.

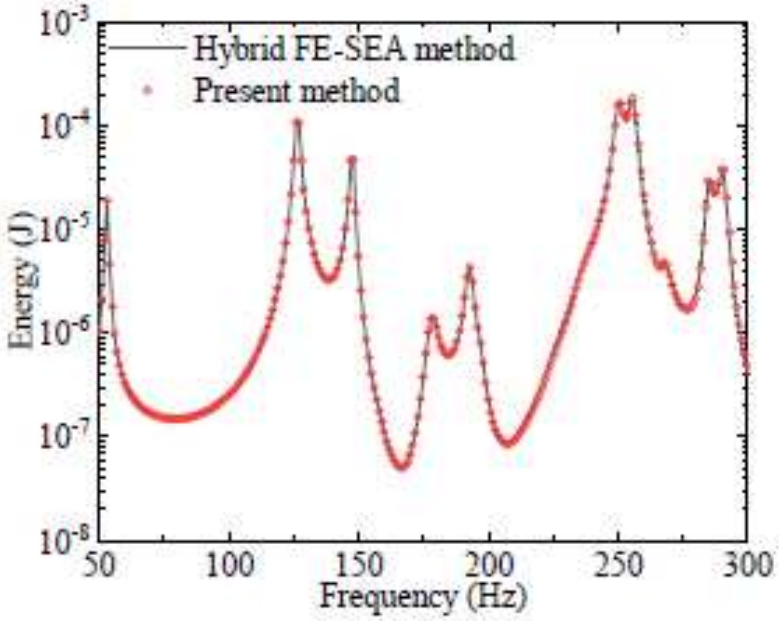

Fig. 6 Energy in panel 4.

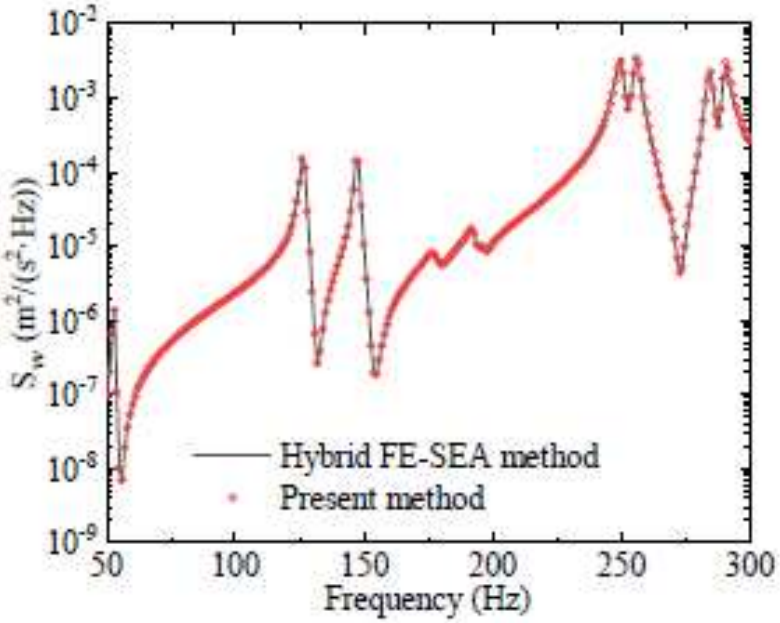

Fig. 7 Modulus squared velocity response at observation point #1.

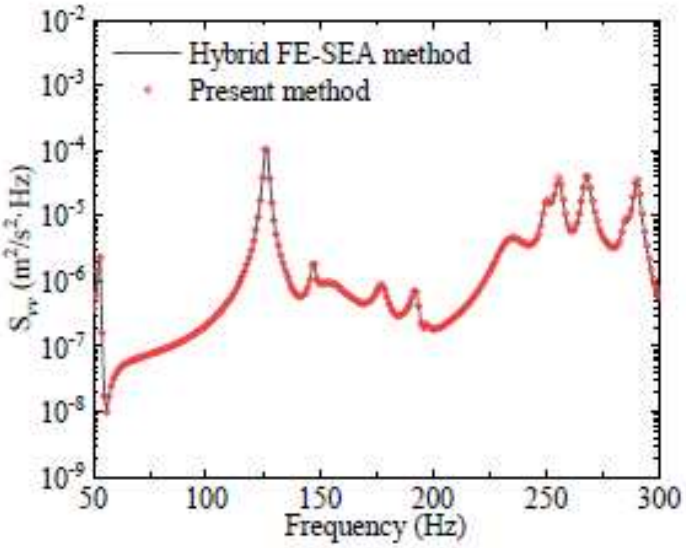

Fig. 8 Modulus squared velocity response at observation point #2.

To verify the efficiency of the proposed method, Table 1 gives the numbers of degrees of freedom and the computation time for the models established by the previous hybrid FE-SEA method and the proposed method, respectively. As given in Table 1, a significant reduction in the computation time can be obtained by using the proposed method. In addition, the computation time increases slowly as the number of included modes increases. It is noted that the implementations were performed by the Julia (v 1.0.1) platform in OS Windows 10 (64 bit) with an Intel Xeon E3-1226, 3.3GHz CPU and 32 GB memory.

Table 1 Model details and the computation time for two methods

Analysis model	Number of DOFs	Computation time (seconds)
Present method	18 (Reduced)	62.3 (100 modes)
		68.1 (150 modes)

		71.9 (200 modes)
		79.4 (250 modes)
Present method without the fast inverse algorithm	18 (Reduced)	1018.1
Previous hybrid FE-SEA method	2852	7534.7

To illustrate the accuracy and convergence of the proposed method, the velocity squared frequency responses at the observation point #2 were calculated under different numbers of truncated modes. Selecting the results obtained using the previous hybrid FE-SEA method as a reference and setting the numbers of the truncated modes to 100, 150, 200 and 250, the absolute relative errors are shown in Fig. 9. As can be seen, the absolute relative errors become smaller as the number of truncated modes increases, illustrating the convergence of the proposed method. In addition, an acceptable accuracy (better than 1%) can be obtained for most frequency points by using 150 truncated modes.

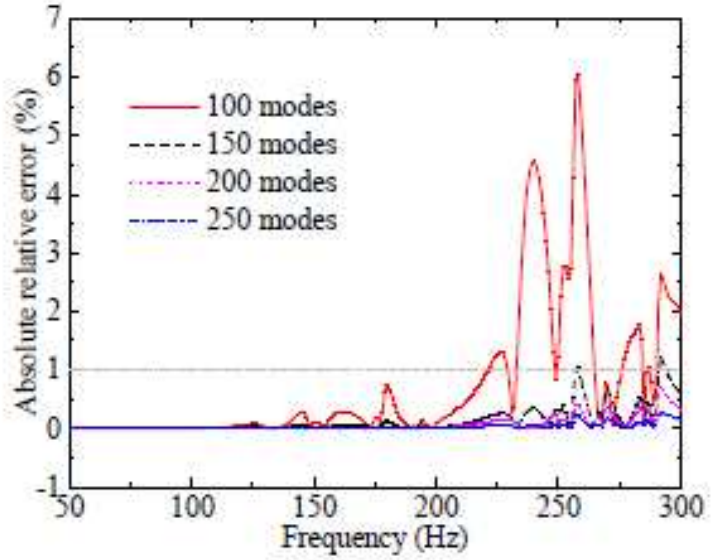

Fig. 9 Absolute relative error of the results obtained under different numbers of truncated modes compared with the reference results.

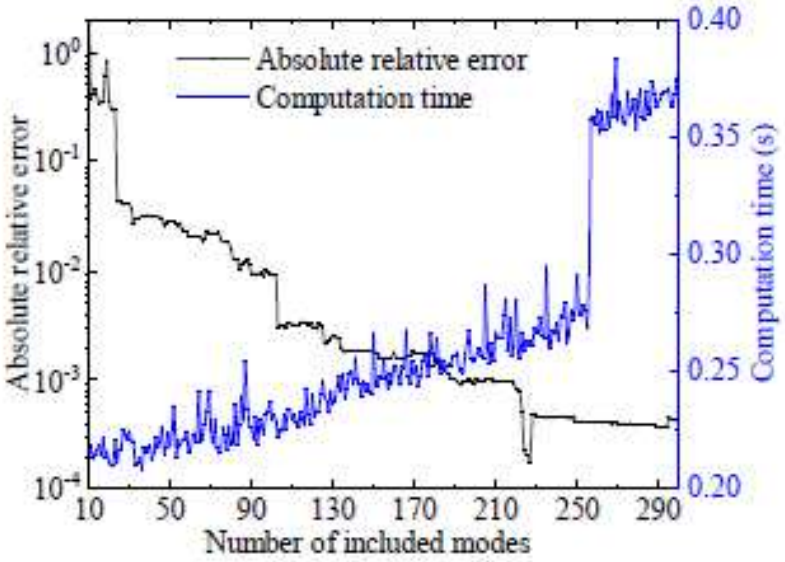

Fig. 10 Convergence of the results obtained by the proposed method.

In order to further study the convergence of the proposed method, a convergence analysis of the modulus squared velocity response at the second observation point #2 is performed. Selecting the frequency as 220Hz, the variation of the absolute relative error and the computation time under different numbers of included modes can be obtained, as shown in Fig. 10. As can be seen, as the number of truncated modes increases, the time cost of the proposed method increases slowly, while the accuracy increases rapidly, which indicates the proposed method has high efficiency and good convergence.

5 Conclusions

The hybrid FE-SEA method requires computation of the total dynamic flexibility matrix at each frequency point, which is very time expensive. This paper presents a strategy to improve the efficiency of the previous hybrid FE-SEA method. In the present method, first, the expensive computation from the inversion of the total dynamic stiffness matrix is transferred to the inversion of the dynamic stiffness matrix of the slave degrees of freedom of the deterministic component generated in the condensation process. Noting that the deterministic component is modelled using the FE method, this inversion is performed using a fast inverse algorithm developed for a pure FE model. The above two steps avoid the direct inverse computation of a large matrix at each frequency, resulting in significant time saving. Compared to the previous hybrid FE-SEA method, the proposed method has higher efficiency and good convergence.

Acknowledgments

The authors are grateful for support under grants from the National Natural Science Foundation of China (11672060), and the Cardiff University Advanced Chinese Engineering Centre.

References

[1] Zienkiewicz OC, Taylor RL. The Finite Element Method. 5th ed. Boston: Butterworth-Heinemann; 2000.

[2] Atalla N, Sgard F. Finite Element and Boundary Methods in Structural Acoustics and Vibration. Boca Raton: CRC Press; 2015.

[3] Lyon RH, DeJong RG. Theory and Application of Statistical Energy Analysis. 2nd ed. Boston: Butterworth-Heinemann; 1995.

[4] Desmet W. Mid-frequency vibro-acoustic modelling: challenges and potential solutions, Proceedings of 2002 International Conference on Noise and Vibration Engineering, ISMA, Leuven, Belgium, 2002, 835-862.

[5] Ladevèze P, Barbarulo A, Riou H, Kovalevsky L. Mid-Frequency - CAE Methodologies for Mid-Frequency Analysis in Vibration and Acoustics. Leuven University Press, Leuven, 2012.

[6] Langley RS. Application of the dynamic stiffness method to the free and forced vibrations of aircraft panels. Journal of Sound and Vibration 1989; 135(2): 319-331.

[7] Bercin AN, Langley RS. Application of the dynamic stiffness technique to the in-plane vibrations of plate structures. Computers and Structures 1996; 59(5): 869-875.

[8] Desmet W. A wave based prediction technique for coupled vibro-acoustic analysis, K. U. Leuven, Division PMA, PhD. Thesis 98D12, 1998; http://www.mech.kuleuven.be /mod/wbm/phd_dissertations/.

[9] Wester ECN, Mace BR. Wave component analysis of energy flow in complex

structures - Part I: A deterministic model. Journal of Sound and Vibration 2005; 285(1-2): 209-227.

[10] Ladevèze P, Arnaud L. New computational method for structural vibrations in the medium-frequency range. Computer Assisted Mechanics and Engineering Sciences 2000; 7(2): 219-226.

[11] Donders S, Pluymers B, Ragnarsson P, Hadjit R, Desmet W. The wave-based substructuring approach for the efficient description of interface dynamics in substructuring. Journal of Sound and Vibration 2010; 329(8): 1062-1080.

[12] Barbarulo A, Ladevèze P, Riou H, Kovalevsky L. Proper Generalized Decomposition applied to linear acoustic: A new tool for broad band calculation. Journal of Sound and Vibration 2014; 333(11): 2422-2431.

[13] Ma Y, Zhang Y, Kennedy D. A symplectic analytical wave based method for the wave propagation and steady state forced vibration of rectangular thin plates. Journal of Sound and Vibration 2015; 339: 196-214.

[14] Nefske DJ, Sung SH. Power flow finite element analysis of dynamic systems: Basic theory and application to beams. Journal of Vibration and Acoustics 1989; 111(1): 94-100.

[15] Langley RS. A wave intensity technique for the analysis of high frequency vibrations. Journal of Sound and Vibration 1992; 159(3): 483-502.

[16] Langley RS, Bercin AN. Wave intensity analysis of high frequency vibrations.

Philosophical Transactions of the Royal Society London A 1994; 346(1681): 489-499.

[17] Maxit L, Guyader JL. Estimation of SEA coupling loss factors using a dual formulation and FEM modal information, Part I: Theory. Journal of Sound and Vibration 2001; 239(5): 907-930.

[18] Maxit L, Guyader JL. Estimation of SEA coupling loss factors using a dual formulation and FEM modal information, Part II: Numerical applications. Journal of Sound and Vibration 2001; 239(5): 931-948.

[19] Wang S, Bernhard RJ. Theory and applications of a simplified energy finite element method and its similarity to SEA. Noise Control Engineering Journal 2002; 50(2): 63-72.

[20] Totaro N, Guyader JL. MODal ENergy analysis. Journal of Sound and Vibration 2013; 332(16): 3735-3749.

[21] Zhao X, Vlahopoulos N. Hybrid finite element formulation for mid-frequency analysis of systems with excitation applied on short members. Journal of Sound and Vibration 2000; 237(2): 181-202.

[22] Shorter PJ, Langley RS. Vibro-acoustic analysis of complex systems. Journal of Sound and Vibration 2005; 288(3): 669-699.

[23] Langley RS, Cordioli JA. Hybrid deterministic-statistical analysis of vibro-acoustic systems with domain couplings on statistical components. Journal of Sound and

Vibration 2009; 321(3-5): 893-912.

[24] Vergote K, Van Genechten B, Vandepitte D, Desmet W. On the analysis of vibro-acoustic systems in the mid-frequency range using a hybrid deterministic-statistical approach. Computers and Structures 2011; 89(11-12): 868-877.

[25] Zhu D, Chen H, Kong X, Zhang W. A hybrid finite element-energy finite element method for mid-frequency vibrations of built-up structures under multi-distributed loadings. Journal of Sound and Vibration 2014; 333(22): 5723-5745.

[26] Ma Y, Zhang Y, Kennedy D. A hybrid wave propagation and statistical energy analysis on the mid-frequency vibration of built-up plate systems. Journal of Sound and Vibration 2015; 352: 63-79.

[27] Gao R, Zhang Y, Kennedy D. A hybrid boundary element-statistical energy analysis for the mid-frequency vibration of vibro-acoustic systems. Computers and Structures 2018; 203: 34-42.

[28] Shorter PJ, Langley RS. On the reciprocity relationship between direct field radiation and diffuse reverberant loading. Journal of the Acoustical Society of America 2005; 117(1): 85-95.

[29] Cotoni V, Shorter PJ, Langley RS. Numerical and experimental validation of a hybrid finite element-statistical energy analysis method. Journal of the Acoustical Society of America 2007; 122(1): 259-270.

[30] Leung AYT. Dynamic Stiffness and Substructures. London: Springer; 1993.

[31] Siemens Product Lifecycle Management Software Inc. NX Nastran User's Guide. Munich: Siemens AG; 2014.